J. Cent. South Univ. (2021) 28: 2269−2284
DOI: https://doi.org/10.1007/s11771-021-4768-9

Springer

Effect of hot extrusion on microstructure and tribological behavior of Al_2O_{3p} reinforced 7075 aluminum-matrix composites

LEI Yu-shun(雷雨顺)[1, 2], YAN Hong(闫洪)[1, 2], WEI Zhi-fan(魏志帆)[1, 2], XIONG Jun-jie(熊俊杰)[1, 2], ZHANG Peng-xiang(张鹏翔)[1, 2], WAN Jian-ping(万剑平)[3], WANG Zhi-lu(王志录)[3]

1. School of Mechanical and Electrical Engineering, Nanchang University, Nanchang 330031, China;
2. Key Laboratory of Light Alloy Preparation and Processing in Nanchang City, Nanchang 330031, China;
3. Jinghang Aviation Forging and Casting Co., Ltd., Jingdezhen 333000, China

Abstract: The effects of hot extrusion and addition of Al_2O_{3p} on both microstructure and tribological behavior of 7075 composites were investigated via optical microscopy (OM), scanning electron microscopy (SEM), energy dispersive spectrometry (EDS), and transmission electron microscopy (TEM). The experimental consequences reveal that the optimal addition of Al_2O_{3p} was 2 wt%. After hot extrusion, the $Mg(Zn,Cu,Al)_2$ phases partially dissolve into the matrix and generate many uniformly distributed aging precipitation particles, the Al_7Cu_2Fe phases are squeezed and broken, and the Al_2O_{3p} become uniform distribution. The microhardness of as-extruded 2 wt% Al_2O_{3p}/7075 composites reaches HV 170.34, increased by 41.5% than as-cast composites. The wear rate of as-extruded 2 wt% Al_2O_{3p}/7075 composites is further lower than that of as-cast composites under the same condition. SEM-EDS analyses reveal that the reinforced wear resistance of composites can put down to the protective effect of the Al_2O_{3p} reinforced transition layer. After hot extrusion, the transition layer becomes stable, which determines the reinforced wear resistance of the as-extruded composites.

Key words: 7075 alloy; Al_2O_{3p}; composites; hot extrusion; microstructure; tribological behavior

Cite this article as: LEI Yu-shun, YAN Hong, WEI Zhi-fan, XIONG Jun-jie, ZHANG Peng-xiang, WAN Jian-ping, WANG Zhi-lu. Effect of hot extrusion on microstructure and tribological behavior of Al_2O_{3p} reinforced 7075 aluminum-matrix composites [J]. Journal of Central South University, 2021, 28(8): 2269−2284. DOI: https://doi.org/10.1007/s11771-021-4768-9.

1 Introduction

Aluminum-matrix composites are materials with strong vitality emerging in response to the development requirement of many industries that composed of Al or its alloys, and various kinds of hard reinforced particles like Al_2O_3, ZrO_2, WC, SiC, B_4C, and Mg_2Si [1−4]. Due to their intrinsic attribute, those reinforced particles can optimize mechanical and physical properties of aluminum alloy [5]. Among the reinforced particles, oxides ceramic particles are frequently applied to aluminum matrix composites due to its stability and inertia, wear resistance, and high temperature resistance [6]. Some researchers have proved that aluminum-matrix composites optimized with oxides ceramic reinforcement possess better mechanical and physical properties, which are extremely suitable for tribological parts by reason of their advanced specific strength, stroke density, lower coefficient of thermal expansion and good wear resistance. BAHRAMI et al [7] synthesized Al/(10Ce-TZP/Al_2O_3) nanocomposite with 7 wt% of

Foundation item: Project(51965040) supported by the National Natural Science Foundation of China; Project(20181BAB206026) supported by the National Science Foundation of Jiangxi Province, China
Received date: 2020-10-26; **Accepted date:** 2021-03-26
Corresponding author: YAN Hong, PhD, Professor; Tel: +86-13667090600; E-mail: hyan@ncu.edu.cn; ORCID: https://orcid.org/0000-0003-1835-3675

reinforcement 10Ce-TZP/Al_2O_3 particles which have a significant improvement in compressive strength compared to the matrix alloy. SAJJADI et al [8] revealed that the microhardness and compressive strength of the composites sample increase, as the weight percentage of Al_2O_{3p} increases. BARADESWARAN et al [9] reported that the proper amount of Al_2O_{3p} and graphite addition increase both microhardness and wear resistance of the hybrid composites.

The common technologies for preparing composites materials include powder metallurgy, melt technology, and extrusion casting technology [10, 11]. Stir casting has been widely used to synthesize discontinuous reinforced aluminum matrix alloy because of its flexibility, simplicity, low expense, and adaptability to mass production [12]. However, the non-uniform distribution and agglomeration, moreover, casting defects such as the formation of porosity and interfacial reactions, arise from the unsatisfactory casting techniques, which minify both microstructure and wear resistance of fabricated composites [13−16]. For the sake of consolidating and improving the particle distribution, secondary processes such as extrusion, forging, or rolling is an effective method to eliminate the casting defects and promote microstructure evenly distributed. Hot extrusion is used as an effective secondary processing due to the remarkable preferential axial alignment of the discontinuous fibers and the large compressive hydrostatic stress state [17]. According to reports, hot extrusion can eliminate casting defects and produce a large number of dislocations during plastic deformation. What's more, hot extrusion can also reduce segregation phenomenon and obtain a uniform distribution of reinforcement particles into the matrix, and sequentially improve the mechanical and physical properties and the wear resistance of aluminum matrix composites. GHANARAJA et al [18] have reported that compressive force during the hot extrusion process reduces the porosity content and matrix grain size, and promotes Al_2O_3 particles evenly distributed. SOLTANI et al [19] have reported that the wear resistance of as-extruded composites has been evidently improved compared to as-cast composites. In the samples extruded at the highest extrusion ratio, it was observed that the tiny Mg_2Si particles hindered plastic deformation, and the weight loss and friction coefficient were the lowest.

There has been a quantity of researches to analyze the tribological behavior characteristics of aluminum matrix composites reinforced by various types and content of reinforcement. However, few attempts have been made to analyze the influences caused by hot extrusion and Al_2O_{3p} ceramic reinforcement particles on 7075 alloy. In the current study, the as-cast and as-extruded Al_2O_{3p}/7075 composites with appropriate addition of Al_2O_{3p} are successfully fabricated. The optical microscopy, scanning electron microscopy with energy dispersive spectrometry and transmission electron microscopy are used to analyze the influence of both the addition of Al_2O_{3p} and hot extrusion on the microstructure, microhardness and tribological behavior characteristics, and analyze the corresponding strengthening mechanism.

2 Experimental

2.1 Materials

In this experiment, the commercial 7075 alloy ingots produced by Minling Metal Materials Co., Ltd., were selected as matrix, and the chemical compositions of 7075 alloy are measured by an ICP, whose main chemical components are shown in Table 1. Al_2O_3 particles (Al_2O_{3p}) produced by Shanghai Yaoyi Alloy Material Co., Ltd., with a particle size of 0.5−1 μm were selected as the particle reinforcement phases. In order to guarantee the same content of other elements in the composites, pure aluminum powders were added into the matrix.

Table 1 Main chemical components of 7075 alloy (wt%)

Zn	Mg	Cu	Mn	Ti	Cr	Si	Fe	Al
5.23	2.10	1.45	0.30	0.16	0.23	0.22	0.22	Bal.

2.2 Fabrication of Al_2O_{3p}/7075 composites

The Al_2O_{3p}/7075 composites were fabricated via a combination of casting and hot extrusion. The schematic illustration is showed in Figure 1. In order to make the Al_2O_{3p} better dispersed in the matrix, the first step of the experiment was to prepared 10 wt% Al_2O_{3p}/7075 preforms by mechanical stirring and ball milling, and then added Al_2O_{3p} into the 7075 alloy by adding the preforms. To remove surface impurities of Al_2O_{3p} and get pure material, certain amounts of Al_2O_{3p} were sonicated in absolute ethyl alcohol for 25 min and then dried in vacuum at 200 °C for 3 h, finally roasted in a furnace at 550 °C

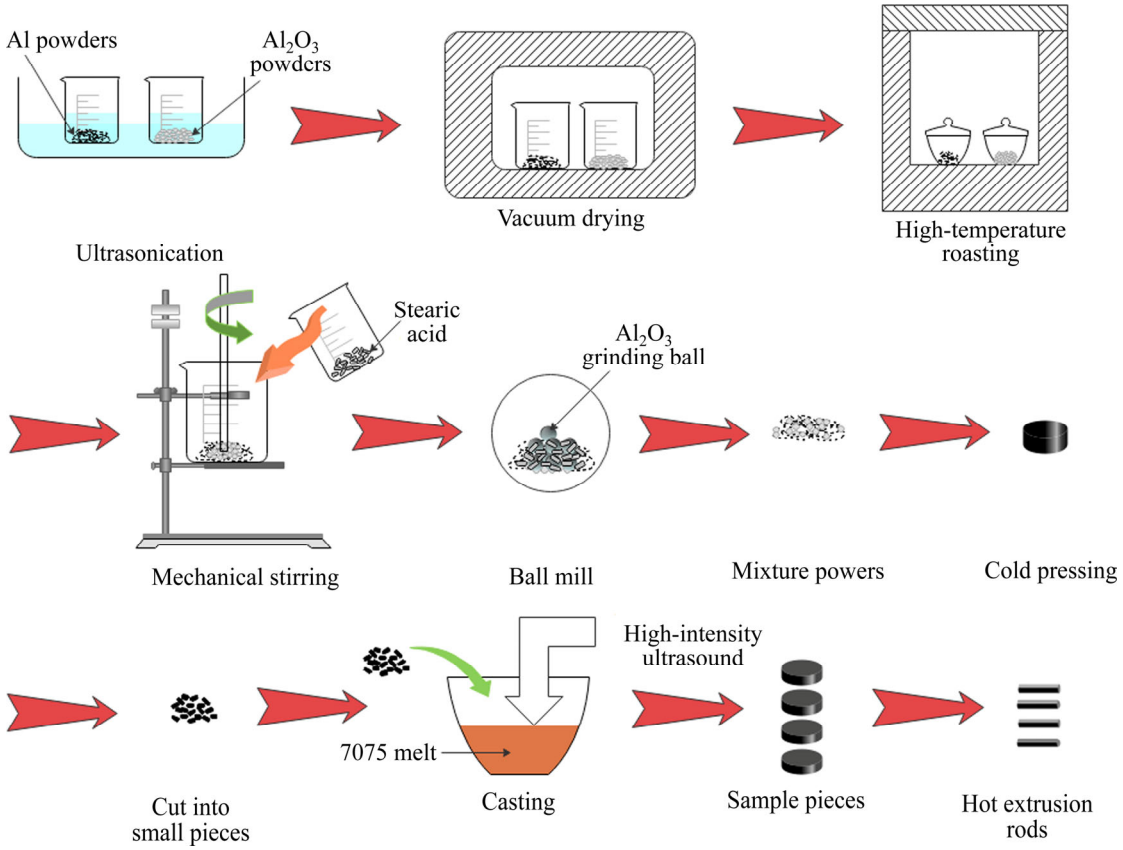

Figure 1 Schematic illustration for synthesizing the Al_2O_{3p}/7075 composites

for 3 h. The mixtures of 10 wt% Al_2O_{3p}/Al powders and 1 vol% stearic acid was mixed via mechanical stirring. And then the mixed powers were milled via a planetary ball mill at 150 r/min for 5 h. The argon gas and stearic acid were used as shielding gas and stabilizer respectively to prevent powders from being oxidized and cold welding, respectively. In order to produce 10 wt% Al_2O_{3p}/7075 preforms, the mixtures were compacted at 400 MPa.

After the preparation of preforms, the second step of the experiment was to prepare the as-cast composites. The 7075 alloy inside the resistance furnace was heated to 780 °C. After the materials melted completely, the liquid alloy was suffered ultrasonic vibration for 10 min at a frequency of 10 kHz and a power level of 2.1 kW. During the ultrasonic vibration process, 10 wt% Al_2O_{3p}/Al preforms as required were added into a melt. After addition, the liquid alloy continued to ultrasonic vibration treatment for 5 min. Subsequently, the liquid alloy was poured into the preheated *d*40 mm metal mold to obtain Al_2O_{3p}/7075 composites containing different addition of Al_2O_{3p} (0, 1 wt%, 2 wt%, and 3 wt%).

After the preparation of as-cast composites, the third step of experiment was to prepare the as-extruded composites. To eliminate casting defects, hot extrusion was used to obtain higher performance composites. The prepared *d*40 mm composites were placed in a vacuum heat treatment furnace, heated to 460 °C, and kept for 2 h. Subsequently, the composites were placed in extrusion die to extrude *d*9 mm rod-shaped extruded specimens. During the extrusion process, the extrusion temperature was 460 °C, the extrusion rate was 2 mm/s, the extrusion ratio was 20:1, and the specimens were cooled by water.

2.3 Characterization

The microstructure evolution was manifested by optical microscope (OM, Nikon MA200), scanning electron microscope (SEM, VEGA3, TESCAN China, Ltd., Shanghai, China) equipped with energy dispersive spectroscopy (EDS) and transmission electron microscopy (TEM, JEM-2100). The microhardness was scaled by the Victorinox (HXS-1000A) tester. The preload was set as 100 N and the preload time was 15 s. Three data were tested repeatedly at each sample.

The tribological behavior was tested in

MMD-1 (Jinan Yihua Tribology Testing Technology Co., Ltd., Jinan, China) by the pin-on-disc device. The composites were processed into *d*4.5 mm× 11 mm pin samples. During the test process, the wear rates were respectively 0.19 and 0.57 m/s, the friction normal loads were respectively 1.3, 2.6 and 3.9 MPa. The real-time friction coefficient during the test was produced from the MMD-1 device. After the test, the pins cleaned in alcohol by ultrasonic vibration for 5 min, and the mass change of the samples weighed by the FA2204B electronic balance. The friction surface of pins was characterized by SEM-EDS.

3 Results and analysis

3.1 Effect of Al_2O_{3p} on 7075 alloy

The microstructure of as-cast Al_2O_{3p}/7075 composites containing different additions of Al_2O_{3p} is displayed in Figure 2. In Figure 2(a), the microstructure of 7075 alloy mainly contains coarse α-Al and dendritic eutectic phases. In Figure 2(b), the α-Al and eutectic phases of 1 wt% Al_2O_{3p}/7075 composite are refined by Al_2O_{3p}, and become more uniform, but the Al_2O_{3p} are locally distributed at grain boundary of 7075 matrixes. When the Al_2O_{3p} content reaches 2 wt%, the distribution of Al_2O_{3p}, as applied in Figure 2(c), is more uniform compared with Figure 2(b). Figure 2(d) manifests a large amount of Al_2O_{3p} aggregation distribution along the grain boundary with 3 wt% Al_2O_{3p} addition. From the above, the optimum addition of Al_2O_{3p} is 2 wt%.

To further confirm the effect of Al_2O_{3p} on 7075 alloy, SEM and EDS were carried out, and the results are shown in Figures 2(e) and (f). According to the research [20, 21], the phases of as-cast Al_2O_{3p}/7075 composites are basically constitutive of Al_7Cu_2Fe, $Mg(Zn,Cu,Al)_2$ and the dominant second phases are the $Mg(Zn,Cu,Al)_2$ phases. Figure 2(e) illustrates the SEM and the EDS images of the as-cast 7075. Combined with the EDS results, the dendritic phases at the grain boundaries are mainly $Mg(Zn,Cu,Al)_2$ and Al_7Cu_2Fe. Additionally, some cracks can be observed at the intersection of grain boundaries in Figure 2(e). These dendritic phases and cracks split the matrix. When the material is stressed, these places will cause stress concentration and reduce mechanical properties. The results of SEM and EDS in 2 wt% Al_2O_{3p}/7075 composites are displayed in Figure 2(f). The microstructure becomes more uniform. The α-Al boundaries become clearer and the $Mg(Zn,Cu,Al)_2$, Al_7Cu_2Fe phases are refined compared with the microstructure of as-cast 7075. Furthermore, the results of EDS illustrate that Al_2O_{3p} mainly distribute at the grain boundaries and agglomerate in some areas. The agglomerated Al_2O_{3p} are poorly bonded to the matrix. When the materials are subjected to shear stress, the agglomerated Al_2O_{3p} are prone to fall off and form pits, causing great damage to the material.

3.2 Effect of hot extrusion on composites

The microstructure of as-extruded 2 wt% Al_2O_{3p}/7075 composites vertical to the extrusion direction is displayed in Figure 3(a). The intermetallic phases are broken and become round. The aggregated Al_2O_{3p} become uniformly distributed in the microstructure. The microstructure of as-extruded 2 wt% Al_2O_{3p}/7075 composites parallel to extrusion direction is shown in Figure 3(b). The intermetallic phases and Al_2O_{3p} change from distribution along grain boundaries to distribution along the extrusion direction. Additionally, the intermetallic phases are crushed into chains under the action of shear force, and the aggregated Al_2O_{3p} become evenly dispersed and distributed along the extrusion direction with other intermetallic phases. The SEM image and the EDS of the as-extruded 2 wt% Al_2O_{3p}/7075 composites parallel to extrusion direction are shown in Figure 3(c), by surface scanning. The EDS results display that the O and Fe elements are parallel to the extrusion direction and extend along the extrusion direction, in addition, the Cu and Zn elements are uniformly distributed. This proves that the Al_7Cu_2Fe phases and Al_2O_{3p} clusters are crushed and broken, and the $Mg(Zn,Cu,Al)_2$ phases have partially dissolved into matrix after the isothermal treatment at 460 °C for 2 h prior to hot extrusion and the process of hot extrusion.

To further confirm the presence and dispersion of Al_2O_{3p} and $Mg(Zn,Cu,Al)_2$ phases, the transmission electron microscope examination were performed in Figures 4(a) and (b). As can be clearly seen in Figure 4(a), the particle is well embedded in the matrix without agglomeration. The EDS analysis of the particles reveal that the main components of the particles were Al and O, and the ratio is corresponding to the Al_2O_3 stoichiometric. Figure 4(b) displays the TEM image and the EDS of

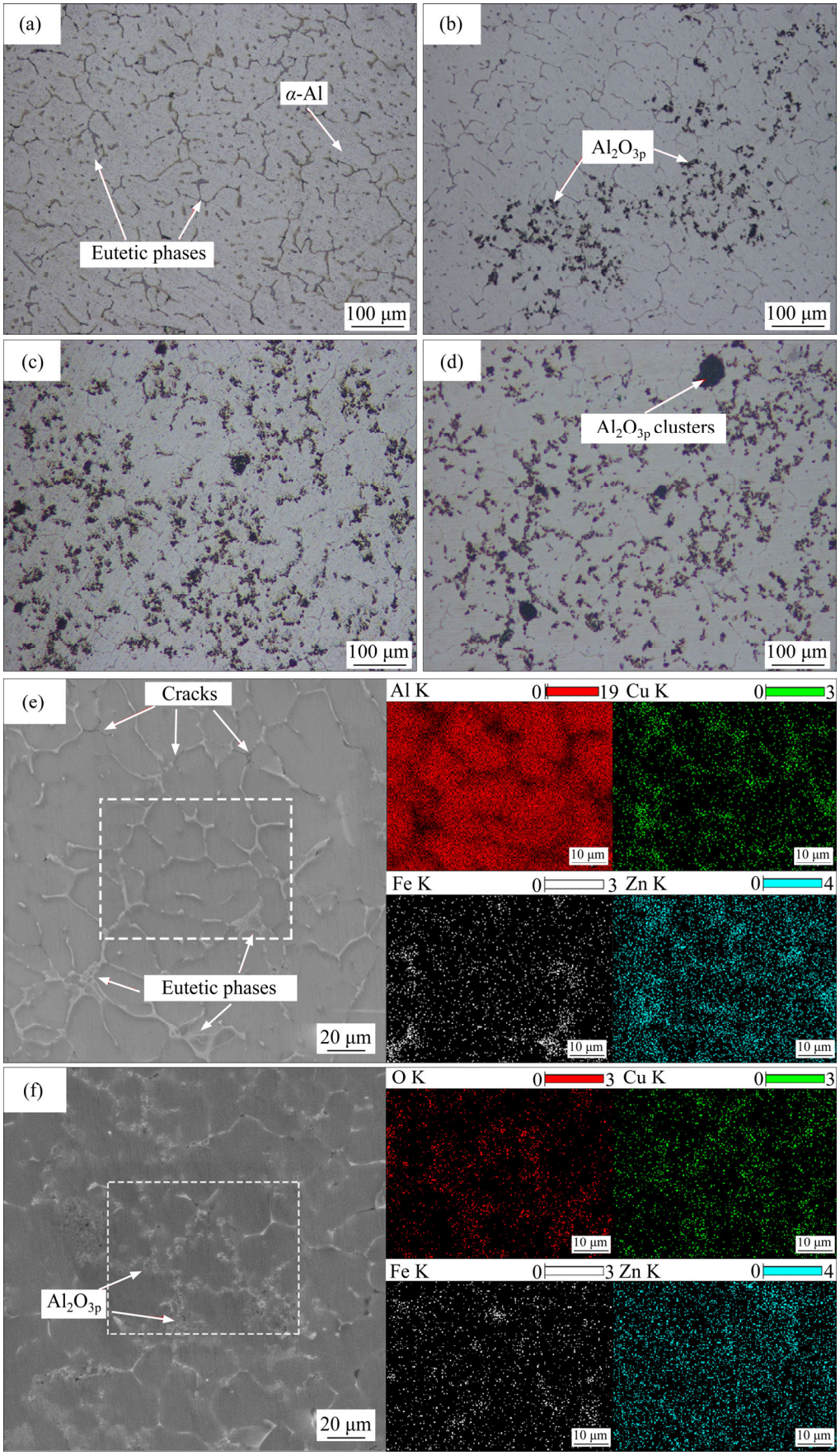

Figure 2 Microstructure of (a) as-cast 7075, (b) 7075+1 wt% Al_2O_{3p}, (c) 7075+2 wt% Al_2O_{3p}, and (d) 7075+3 wt% Al_2O_{3p}; SEM images and EDS results by surface scanning of (e) as-cast 7075 alloy and (f) 2 wt% Al_2O_{3p}/7075 composites

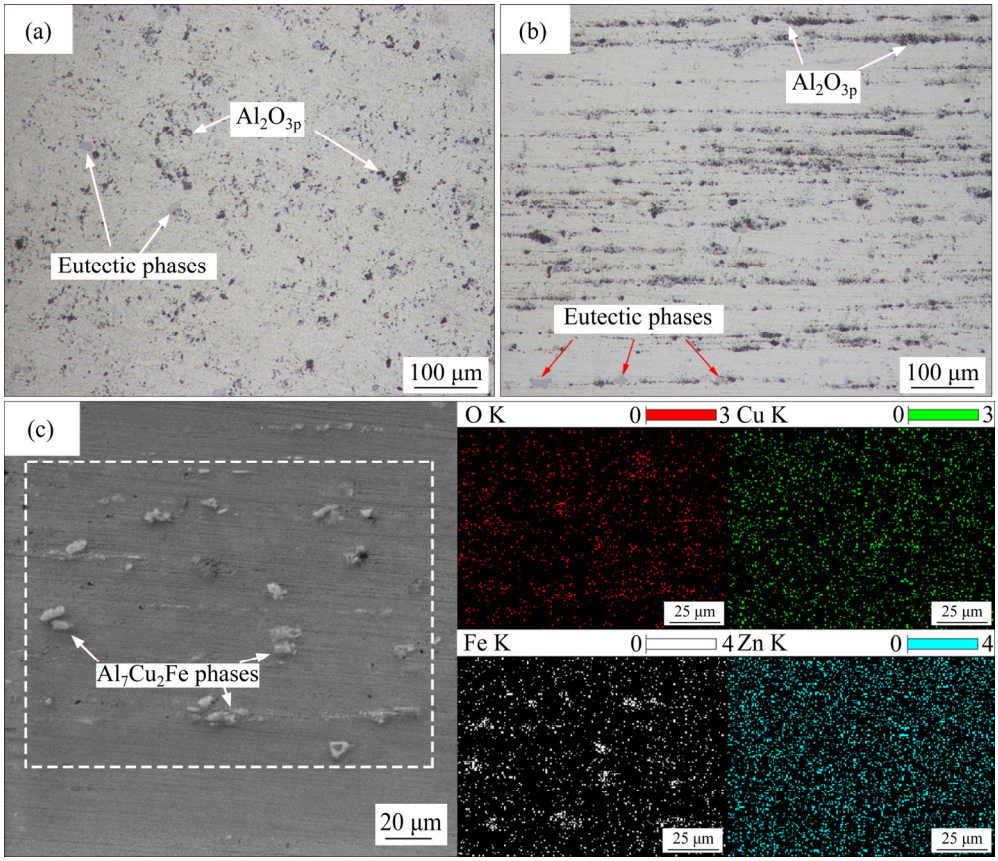

Figure 3 Microstructure of as-extruded 2 wt% Al_2O_{3p}/7075 composites: (a) Vertical to extrusion direction; (b) Parallel to extrusion direction; (c) SEM image and EDS of as-extruded 2 wt% Al_2O_{3p}/7075 composites parallel to extrusion direction

the aging precipitation phases in the matrix. The EDS results illustrate that the precipitated phases mainly contains Zn, Cu, and Mg elements, which suggests the precipitated phases are $Mg(Zn,Cu,Al)_2$ phases. After hot extrusion, the dendritic $Mg(Zn,Cu,Al)_2$ phases dissolve into the matrix, and then precipitate, generating a large number of uniformly distributed fine $Mg(Zn,Cu,Al)_2$ phases.

3.3 Microhardness analysis

The microhardness of as-cast and as-extruded composites containing various addition of Al_2O_{3p} are displayed in Figure 5. After adding Al_2O_{3p}, the microhardness of as-cast alloy is significantly improved. The microhardness of as-cast 2 wt% Al_2O_{3p}/7075 reaches the maximum value (HV 120.34), and increased by 23.3% compared to that of as-cast 7075 matrix alloy. When the addition of Al_2O_{3p} is 3 wt%, the microhardness of as-cast composites decreases compared to that of the former. Al_2O_{3p} as ceramic reinforced particles can improve the hardness of alloy. Combined with the microstructure of as-cast 7075 alloy, the Al_2O_{3p} refine the grain and the second phase, which suggests that Al_2O_{3p} can enhance the microhardness of the matrix. In addition, the thermal expansion coefficient of Al_2O_{3p} (7.8 μm/K) and 7075 alloy (24.5 μm/K) are greatly different [22]. These will produce thermal mismatch stress and generate dislocations at the boundary of Al_2O_{3p} and α-Al after the process of fabrication and cooling of composites. A large number of dislocations are clustered and entangled at the grain boundary, creating interactions that impede the dislocation motion and lead to reinforcement of the composites [23]. Most of the agglomeration would destroy the integrity of microstructure, and cause potentially stress concentration, reducing the property of composites. When excessive Al_2O_{3p} is added, Al_2O_{3p} agglomerate in the matrix, leading to the microhardness displays a decreasing trend.

After hot extrusion, the microhardness of as-extruded composites is further increased compared to the as-cast composites. The microhardness of as-extruded 2 wt% Al_2O_{3p}/7075 composites reaches HV 170.34, which is 41.5%

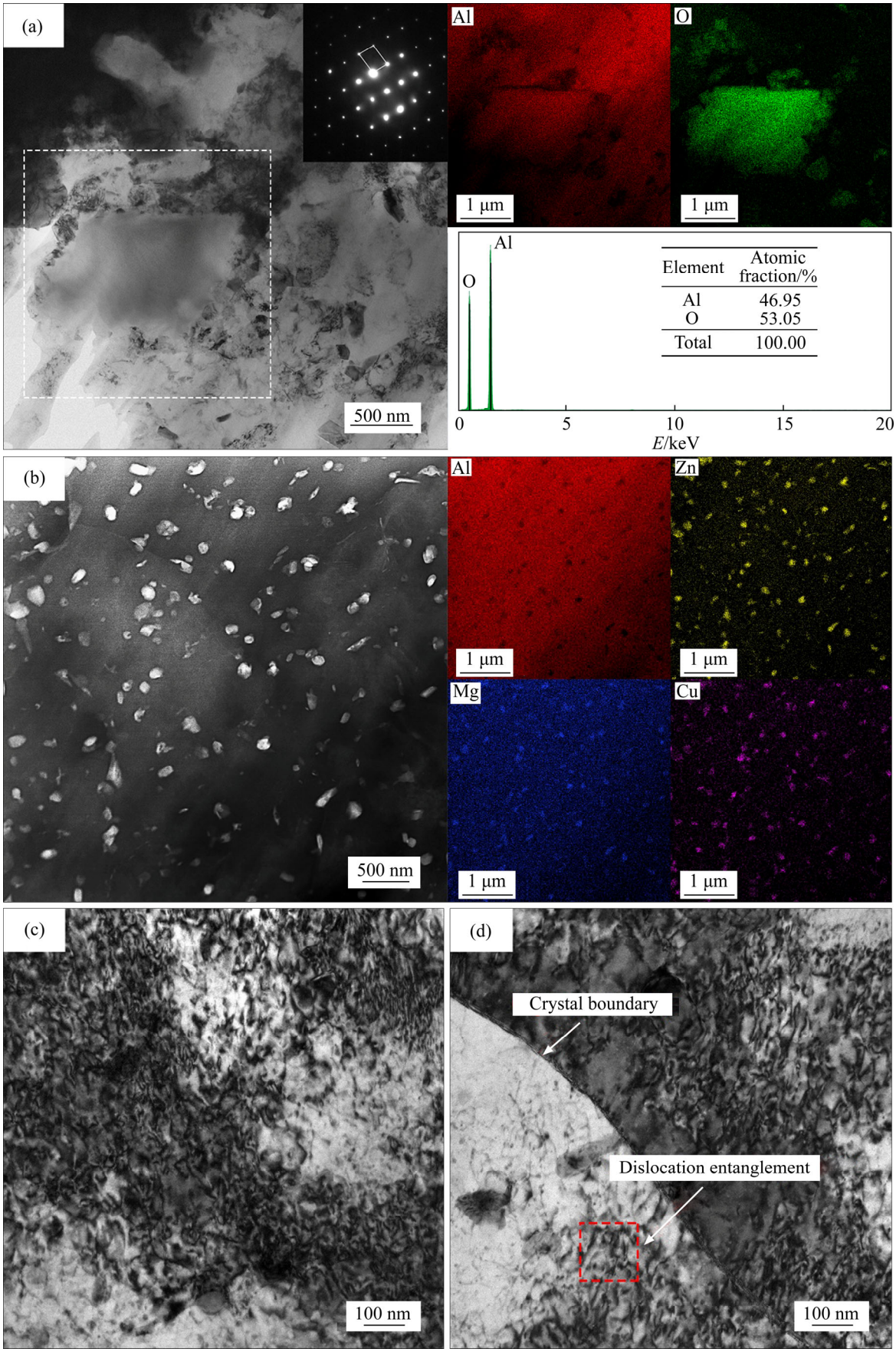

Figure 4 TEM images of 2 wt% Al_2O_{3p}/7075 composites: (a) Al_2O_{3p}; (b) $Mg(Zn,Cu,Al)_2$ phases; (c) Dislocations in grain; (d) Dislocations at crystal boundary

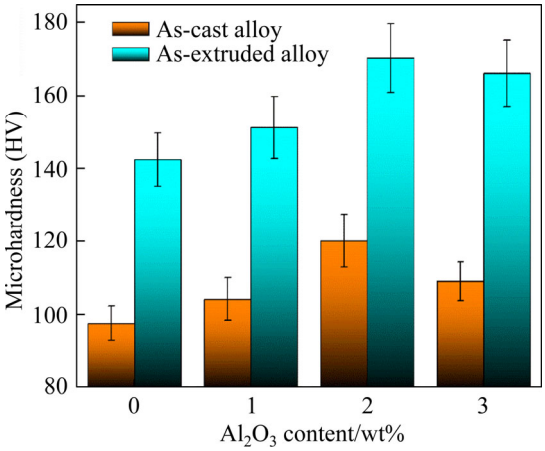

Figure 5 Microhardness of as-cast and as-extruded composites with different Al_2O_{3p} contents

higher than that of the as-cast 2 wt% Al_2O_{3p}/7075 composites. Hot extrusion eliminates casting defects in the composites. When the liquid alloy solidifies, casting defects such as thermal cracking, shrinkage cavity will occur due to volume shrinkage and gas evolution, which will become the source of cracks in the alloy fracture. Hot extrusion can weld and eliminate most casting defects in the composites. Additionally, hot extrusion causes the agglomerated Al_2O_{3p} to disperse evenly due to its the excellent preferential axial alignment of discontinuous fibers as well as large compressive hydrostatic stress state [17], which effectively improves the properties of the composites.

During hot extrusion process, huge deformation occurs in the grain and produce a mass of dislocations as shown in Figure 4(c). These dislocations are principally generated by dislocation slipping, cross slipping, climbing and other ways [24]. Dislocation motion is hindered at the grain boundary, and then forms the high-density dislocation area with irregular dislocation network and entanglement by interaction and cross entanglement as shown in Figure 4(d). The entangled dislocation network at the grain boundary hinders a further deformation of the grain. In addition, the isothermal treatment at 460 °C for 2 h prior to hot extrusion and the process of hot extrusion make $Mg(Zn,Cu,Al)_2$ partially dissolve into the 7075 matrix, and generate many $Mg(Zn,Cu,Al)_2$ nanoparticles after the precipitation process. The $Mg(Zn,Cu,Al)_2$ nanoparticles precipitated in the crystal grain and the stress field around it will hinder the dislocation motion, increase the resistance to deformation, and thus increase the strength of the composites.

3.4 Wear rate analysis

The wear rate is an important parameter to characterize the wear of materials. In this paper, wear rate is defined as the weight loss per unit sliding distance which is calculated by formula (1), as follows:

$$R_w = W/L \quad (1)$$

where R_w denotes the wear rate, W is the mass loss, and L is the sliding distance.

The wear rate of as-cast and as-extruded Al_2O_{3p}/7075 composites variation versus the Al_2O_{3p} content at a sliding distance of 171 m (equivalent to 900 s×0.19 m/s) are displayed in Figure 6. The wear rates of as-cast Al_2O_{3p}/7075 composites with different Al_2O_{3p} contents under different loads are shown in Figure 6(a). With the Al_2O_{3p} content increasing, the wear rate tends to decrease first and then increase. The trend is particularly obvious as the load increases. The change of wear rate can be attributed to the formation of the Al_2O_{3p} reinforced transition layer on the friction pair surface, which not only improves the surface microhardness of composites but also reduces the wear of the matrix [25−27]. When the addition of Al_2O_{3p} reaches 2 wt%, the wear rate reaches the minimum value (0.0234, 0.0398, 0.0614 g/mm) under different loads (1.3, 2.6, 3.9 MPa), which are lower than 7075 alloy (40.3%, 63.2%, 64.5%). Apparently, the 2 wt% Al_2O_{3p}/7075 composites represent excellent wear resistance under the same applied load. When the addition of Al_2O_{3p} is less than 2 wt%, Al_2O_{3p} as reinforced phases can availably bear the normal load and form a three-body friction system. On the one hand, the wear ability of composites is affected by the physical, and chemical property, mechanical property, and high-temperature property of composites; on the other hand, the combination, compatibility, and wettability between the reinforced phase particles and the material also affect the wear ability [28−30]. When the addition of Al_2O_{3p} reaches 3 wt%, the excess Al_2O_{3p} can not be uniformly dispersed in the matrix, which is clustered at the grain boundary. In the friction process, the agglomerated particles are prone to peel off under the action of shear stress and can not form a stable transition layer on the friction surface, causing severe wear.

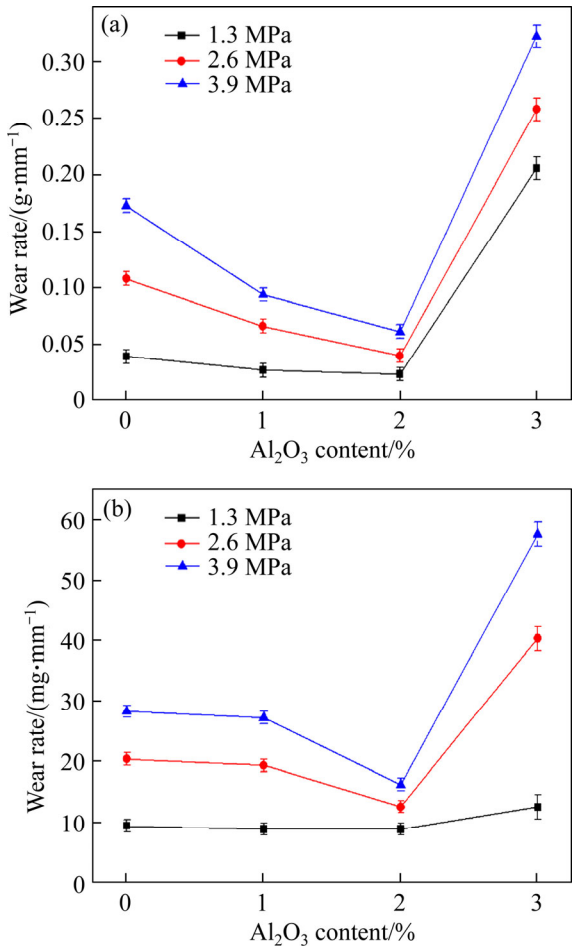

Figure 6 Wear rate of as-cast (a) and as-extruded (b) Al_2O_{3p}/7075 composites variation versus the Al_2O_{3p} content

The wear rates of as-extruded Al_2O_{3p}/7075 composites with different Al_2O_{3p} contents under different loads are shown in Figure 6(b). The wear rate of as-extruded composites is much lower than that of the as-cast composites. Under the 1.3 MPa normal load, the wear rate of as-extruded composites does not change significantly with the increase of Al_2O_{3p} content. This is because, the shear stress on the friction surface is relatively small under the 1.3 MPa normal load, and the wear resistance mainly depends on the mechanical strength of the material [31]. After hot extrusion, the microhardness of the composites has been greatly improved. The wear rate does not change significantly. When the applied load reaches 2.6 and 3.9 MPa, the wear rate of as-extruded Al_2O_{3p}/7075 composites changes significantly. When the Al_2O_{3p} content reaches 1 wt%, the wear rate is lower than that of as-extruded 7075 alloy, but the change is not much. When the Al_2O_{3p} content reaches 2 wt%, the wear rate of composites reduces quickly to the lowest 12.56 and 16.23 mg/mm, which are 38.46% and 42.59% lower than as-extruded 7075 alloy. However, when the Al_2O_{3p} content reaches 3 wt%, the wear rate of composites rises sharply. Excessive Al_2O_{3p} damage the wear resistance of composites and this trend becomes more obvious as the load increases. This finding suggests that the as-extruded Al_2O_{3p}/7075 composites are not sensitive to the content of Al_2O_{3p} under low normal load. 2 wt% Al_2O_{3p}/7075 composites exhibit the best wear resistance under a high normal load.

3.5 Coefficient of friction analysis

The average coefficients of friction (COF) of as-cast and as-extruded composites are displayed in Figure 7. According to the result, the Al_2O_{3p} can reduce the COF of as-casting and as-extruded composites, and 2 wt% Al_2O_{3p}/7075 composites has the lowest COF under the same load, which can help prove why 2 wt% Al_2O_{3p}/7075 has the lowest wear rate. During the friction process, the Al_2O_{3p} do micro-rolling between the friction pairs, which not only changes the sliding friction into rolling and

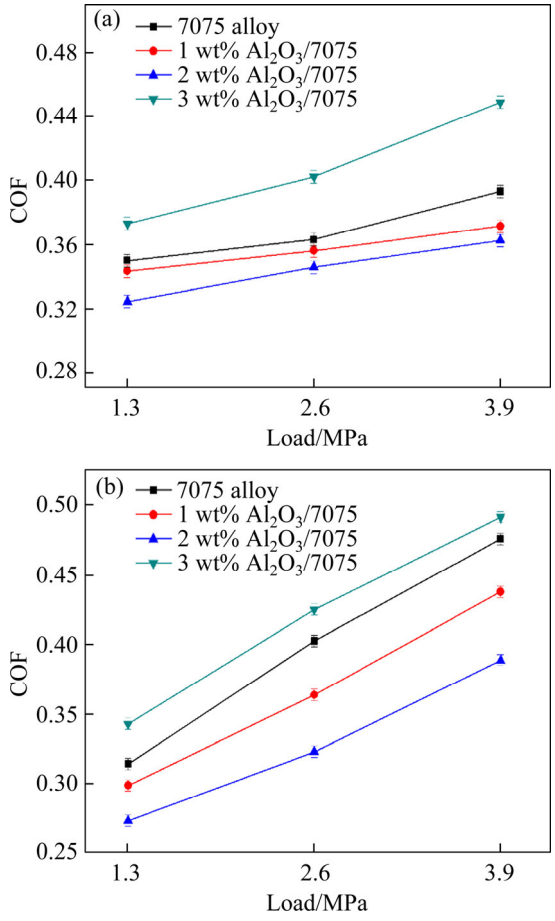

Figure 7 Average COF of as-cast (a) and as-extruded (b) Al_2O_{3p}/7075 composites variation versus Al_2O_{3p} content

sliding composites friction but also makes the two rough contact surfaces not directly contact [32]. When the Al_2O_{3p} content reaches 3 wt%, the excessive Al_2O_{3p} will not only affect the formation of the transition layer but also form larger agglomerated debris particles during the friction process. Under pressure, the agglomerated particles produce furrows on the friction pair, which ultimately manifests as an increase in friction coefficient and wear rate.

The COF of composites increases with the normal load and the COF of as-extruded composites significantly increases faster than as-cast composites. Under the 1.3 MPa normal load, the COF of as-extruded composites is lower than that of the as-cast composites. However, the COF of the as-extruded composites is higher than that of the as-cast composites under the 3.9 MPa normal load. The causes of the above phenomena may be caused by changes in the contact between the disc and sample. When the friction pair are in contact, as implied in Figure 11(a), the contact surface is composed of uneven and discrete rough peaks. With the load increasing, the contact surface undergoes plastic deformation, which increases the actual contact area so that the frictional resistance in the friction direction increases and causes the COF to increase [33]. Compared with as-cast composites, as-extruded composites have higher strength. Under the 1.3 MPa normal load, the microstructure of the friction surface is hard to fall off, so the as-extruded composites has a smoother friction surface, and the actual contact area is small. This leads to a lower COF. However, when the normal load reaches 3.9 MPa, the actual contact area becomes larger, and more rough peaks are contacted gradually. The rough peaks in the as-cast composites friction pairs are easily removed from the contact surface under force and the friction pair can not form a stable contact. The falling off rough peaks roll on the friction surface and reduce the COF. However, these rough peaks of the as-extruded composites are combined firmly with the matrix and able to resist higher frictional resistance. These rough peaks hinder the movement of the friction pair, which is manifested as an increase of COF.

The real COF of as-cast and as-extruded 2 wt.% Al_2O_{3p}/7075 composites, sliding test in 1.3, 2.6, 3.9 MPa normal load, are shown in Figure 8. The as-extruded composites COF amplitude is obviously smaller than that of the as-cast composite, and this phenomenon becomes more obvious as the load and the velocity increases. This is because the friction surface strength of the as-cast composites is low, and the rough peaks in the friction surface easily fall off during the friction process, which results in no stable contact between the friction pairs. The strength of the as-extruded composites is high, and there is a stable contact between the friction pairs during the friction process, which makes the amplitude smaller.

3.6 Wear surface analysis

The wear surface of as-cast and as-extruded 2 wt% Al_2O_{3p}/7075 composites, sliding tested in 1.3 and 3.9 MPa normal load at 0.19 and 0.57 m/s speed, are shown in Figure 9. Under 1.3 MPa normal load and 0.19 m/s speed, as implied in Figure 9(a), the as-cast composites show ploughs, pits, deformation zones, and relatively wide wear grooves on the wear surface, which indicates a mechanism of abrasive and adhesive. In contrast, as shown in Figure 9(b), the surface of the extruded composites exhibits slight scratches and tolerably flat surfaces. These morphologies manifest characteristics of abrasive wear mechanism for the as-extruded composites verify the lower mass loss compared with that of the as-cast composites at an applied load less than 1.3 MPa. As the sliding speed increases to 0.57 m/s, the worn surface for the as-cast composites deteriorates which exhibits more and larger pits and delamination area on the wear surface, as shown in Figure 9(c), indicating the predominant wear mechanism tends to be adhesive. However, in Figure 9(d), the as-extruded composites are not sensitive to the sliding velocity, which still reveal narrower scratches and nearly flat surfaces, indicating a mechanism of abrasive. With the applied load increasing to 3.9 MPa, the wear surfaces of as-cast and as-extruded composites all deteriorate, as displayed respectively in Figures 9(e) and (f). The worn surface of as-cast composites exhibits cracks, grooves and large areas of delaminated layers along the sliding direction. In addition, the EDS analyses of the groove and the smooth area at the wear surface are shown in Figures 10(a) and (b). The elements of point *A* at the groove are close to those of the as-cast 7075 alloy, while the elements of point *B* at the smooth area are Al, O, Fe, Mg and Zn. This result implies that the surface of the transition layer is oxidized and an oxide layer is formed. The wear surface of as-extruded 2 wt% Al_2O_{3p}/7075

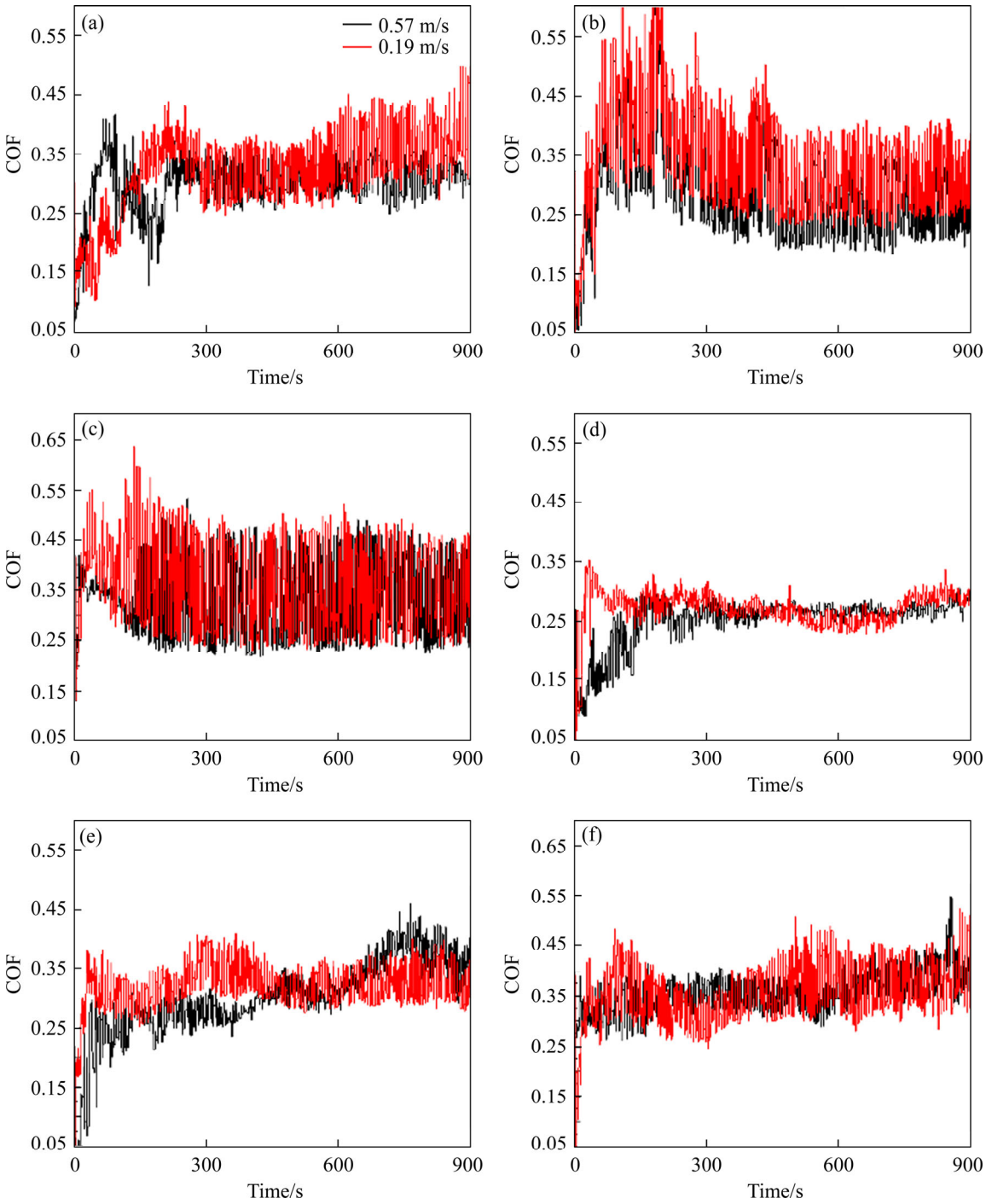

Figure 8 Real COF of as-cast 2 wt% Al_2O_{3p}/7075 composites: (a) 1.3 MPa normal load; (b) 2.6 MPa normal load; (c) 3.9 MPa normal load, and as-extruded 2 wt% Al_2O_{3p}/7075 composites: (d) 1.3 MPa normal load; (e) 2.6 MPa normal load; (f) 3.9 MPa normal load

composites is illustrated in Figure 9(f). Although there are some ploughs and pits on the wear surface, the wear surface is mainly characterized by abrasive wear. The EDS analysis at point *C* is shown in Figure 10(c). The elements of point *C* are O and Al, and the atomic ratio is close to 1.5, which shows that point *C* is Al_2O_{3p}. After hot extrusion, Al_2O_{3p} are evenly distributed in the matrix, improving interface bonding strength between the particles and matrix. During the friction process, the Al_2O_{3p} are difficult to fall off, so there is no serious adhesive wear like as-cast composites.

To further research the difference in wear mechanisms, the morphology of wear debris for as-cast and as-extruded composites containing 2 wt% Al_2O_{3p} tested at 3.9 MPa and 0.19 m/s are

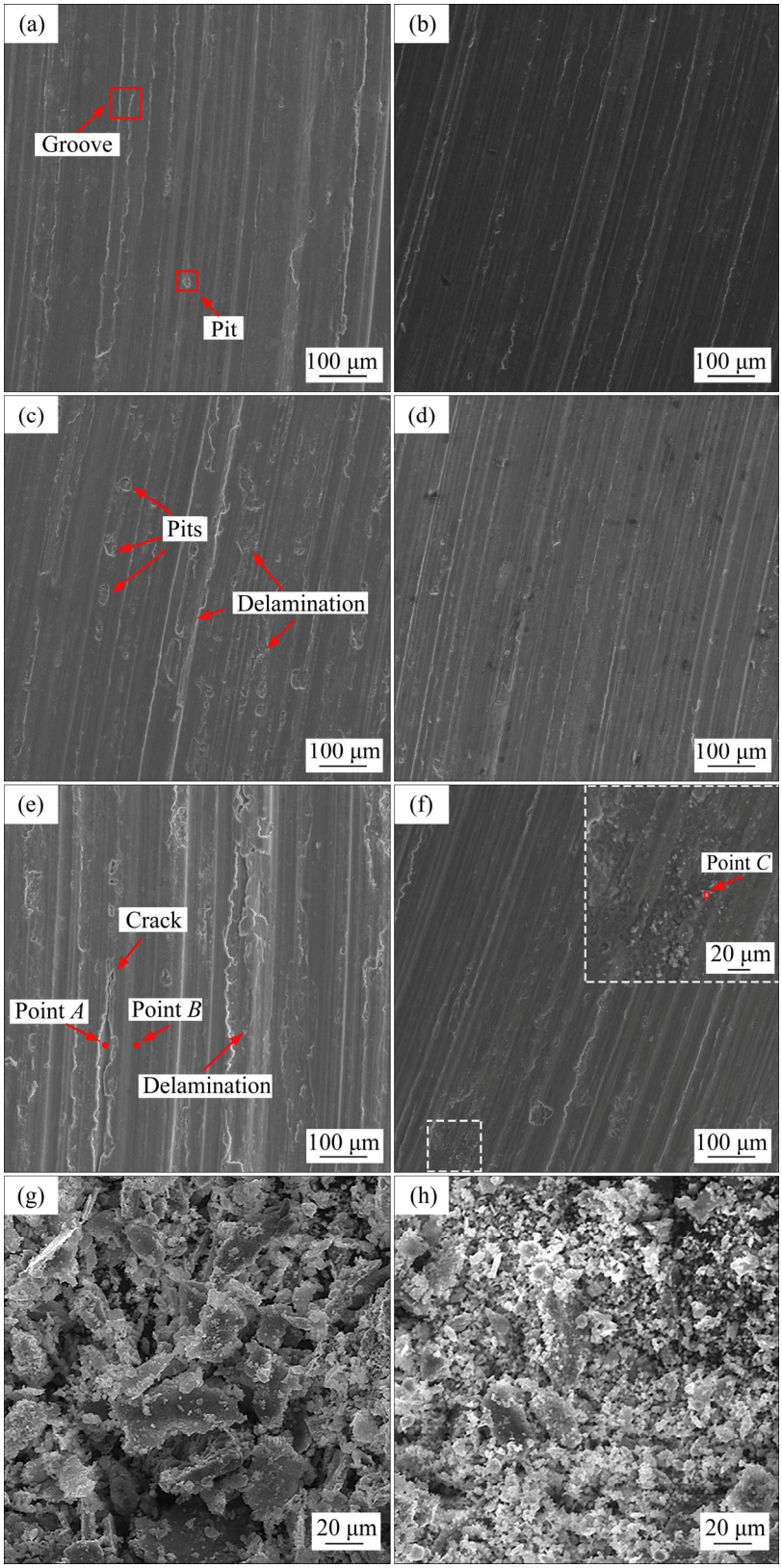

Figure 9 SEM images of wear surface for as-cast 2 wt% Al_2O_{3p}/7075 composites subjected to: (a) 1.3 MPa normal load + 0.19 m/s sliding velocity; (c) 1.3 MPa normal load + 0.57 m/s sliding velocity; (e) 3.9 MPa normal load + 0.19 m/s sliding velocity; as-extruded 2 wt% Al_2O_{3p}/7075 composites subjected to: (b) 1.3 MPa normal load + 0.19 m/s sliding velocity; (d) 1.3 MPa normal load + 0.57 m/s sliding velocity; (f) 3.9 MPa normal load + 0.19 m/s sliding velocity; SEM images of wear debris for as-cast (g) and as-extruded (h) 2 wt% Al_2O_{3p}/7075 composites subjected to 3.9 MPa normal load + 0.19 m/s sliding velocity

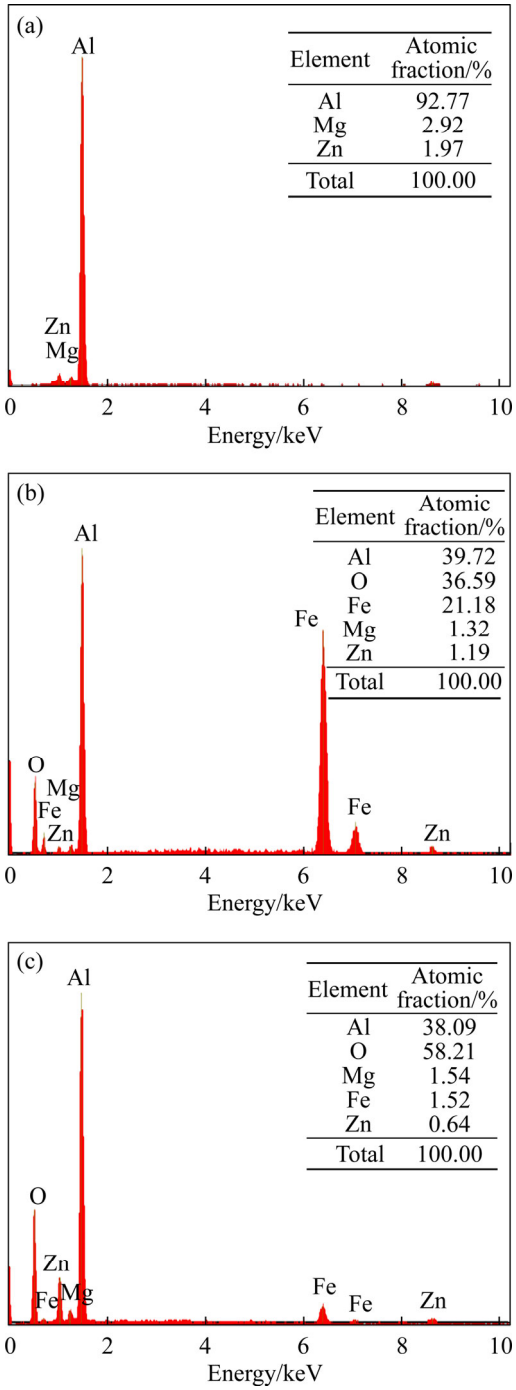

Figure 10 EDS analysis of points *A* (a), *B* (b) and *C* (c) in Figure 9

acquired, as displayed in Figures 9(g) and (h). The wear debris of as-cast composites exhibits block-like morphology of non-uniform dimensions, as shown in Figure 9(g), indicating a mechanism of adhesive. The wear debris of as-extruded composites mainly comprises fine particles, as shown in Figure 9(h). After hot extrusion, the transition layer becomes stable and is difficult to cause serious wear, which determines the size of wear debris. The decrease in the size of wear debris also weakens the ploughing effect between friction pairs. The morphology indicates that the predominant wear mechanism is abrasive wear.

3.7 Wear mechanisms analysis

To further understand the wear mechanisms of as-cast and as-extruded composites during the dry sliding, a diagrammatic sketch of changes in the wear surface is illustrated in Figure 11. Figures 11(a) and (b) displayed the as-cast and as-extruded composites before the test, respectively. There are cracks, intermetallic phases, and Al_2O_{3p} along the grain boundary of the as-cast composites, which tear the matrix and reduce the mechanical. In contrast, the microstructure of as-extruded composites comprises catenary intermetallic phases and evenly dispersed Al_2O_{3p}. During the dry sliding wear test, the wear surface of the as-cast and as-extruded composites produce and aggregate different sizes of wear debris, respectively, as shown in Figures 11(c) and (d). Apparently, the wear debris size of as-cast composites is larger than that of as-extruded composites. This may be due to the fact that the composites are prone to damage from casting defects during the friction process. Figures 11(e) and (f) show the compaction of agglomerates wear debris and the formation of a protective oxide layer. For the wear process of as-extruded composites, the transition oxide layer constitutes smaller debris, which is more stable and have better wear resistance.

4 Conclusions

In the current study, the microstructure, microhardness and the tribological behavior characteristics were investigated. The results indicate that the addition of Al_2O_{3p} can optimize the microstructure of as-cast 7075 alloy, and the optical addition of Al_2O_{3p} is 2 wt%. The primary α-Al becomes uniform and orderly, and the $Mg(Zn,Cu,Al)_2$, Al_7Cu_2Fe phases are refined. After hot extrusion, the $Mg(Zn,Cu,Al)_2$ phases partially dissolved into the matrix. Under extrusion stress, the Al_7Cu_2Fe phases are squeezed and broken, and the aggregated Al_2O_{3p} become evenly dispersed. The microhardness of as-extruded 2 wt% Al_2O_{3p}/7075 composites reaches HV 170.34, which is 41.5% higher than that of the as-cast 2 wt% Al_2O_{3p}/7075 composites.

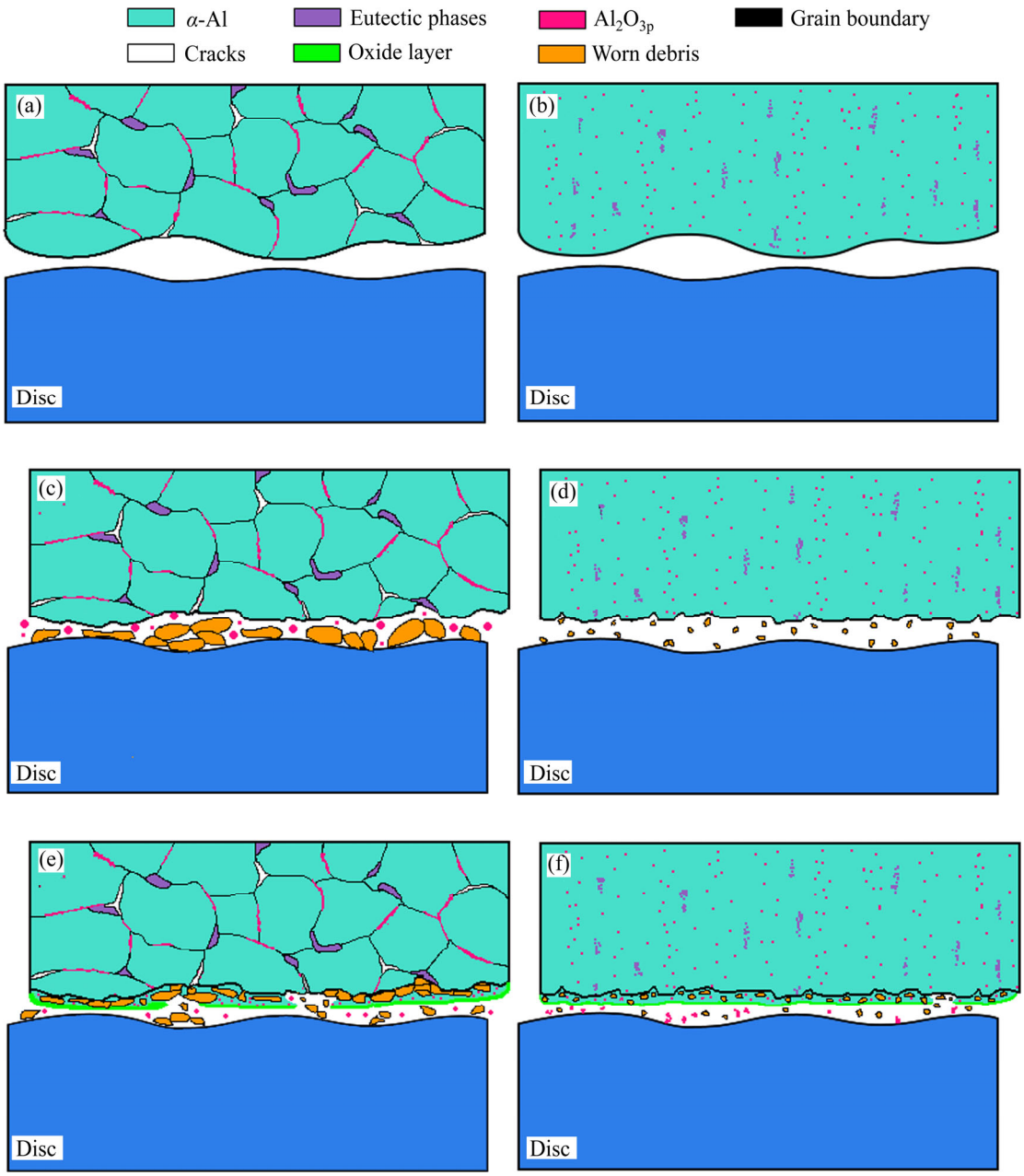

Figure 11 Diagrammatic sketch of changes in wear surface during wear test of as-cast (a, c, e) and as-extruded (b, d, f) composites

The as-cast and as-extruded composites showed different tribological behavior characteristics in the wear test, which indicates that, compared with as-cast composites, as-extruded composites have a further lower wear rate. With the normal load increasing, the wear rate and the COF of both as-cast and as-extruded composites increase, and the real time COF of as-extruded composites is more stable. Protective transition layers are formed on the wear surface of both as-cast and as-extruded composites during the dry sliding process. The protective transition layers of the composites are enhanced by the Al_2O_{3p} and generate better wear resistance for the composites. After the hot extrusion process, the interface bonding strength between the Al_2O_{3p} and the matrix improves and the transition layers become more stable.

Contributors

The overarching research goals were developed by YAN Hong, LEI Yu-shun and WEI Zhi-fan. LEI Yu-shun and WEI Zhi-fan provided the measured microstructure and tribological behavior data, and analyzed the measured data with XIONG Jun-jie and

ZHANG Peng-xiang. WAN Jian-ping and WANG Zhi-lu have provided the corresponding materials and equipment. The initial draft of the manuscript was written by LEI Yu-shun, WEI Zhi-fan. All authors replied to reviewers' comments and revised the final version.

Conflict of interest

LEI Yu-shun, YAN Hong, WEI Zhi-fan, XIONG Jun-jie, ZHANG Peng-xiang, WAN Jian-ping and WANG Zhi-lu declare that they have no conflict of interest.

References

[1] SOLTANI N, PECH-CANUL M I, BAHRAMI A. Effect of 10Ce-TZP/Al_2O_3 nanocomposite particle amount and sintering temperature on the microstructure and mechanical properties of Al/(10Ce-TZP/Al_2O_3) nanocomposites [J]. Materials and Design, 2013, 50: 85−91. DOI: 10.1016/j.matdes.2013.03.001.

[2] SOLTANI N, BAHRAMI A, PECH-CANUL M I. The effect of Ti on mechanical properties of extruded in-situ Al-15 pct Mg_2Si composite [J]. Metallurgical and Materials Transactions A, 2013, 44: 4366−4373. DOI: 10.1007/s11661-013-1747-2.

[3] KALA H, MER K, KUMAR S A. A Review on mechanical and tribological behaviors of stir cast aluminum matrix composites [J]. Procedia Materials Science, 2014, 6: 1951−1960. DOI: 10.1016/j.mspro.2014.07.229.

[4] TENG Jie, Li Hua-pei, CHEN Gang. Wear mechanism for spray deposited Al-Si/SiC_p composites under dry sliding condition [J]. Journal of Central South University, 2015, 22(8): 2875−2882. DOI: 10.1007/s11771-015-2820-3.

[5] DEAQUINO L R, SOLTANI N, BAHRAMI A, GUTIERREZ C E, GARCIA S E, HERNANDEZ R M A L. Tribological characterization of Al7075–graphite composites fabricated by mechanical alloying and hot extrusion [J]. Materials and Design, 2015, 67: 224−231. DOI: 10.1016/j.matdes.2014.11.045.

[6] BAHRAMI A, SOLTANI N, PECH-CANUL M I. Effect of sintering temperature on tribological behavior of Ce-TZP/Al_2O_3-aluminum nanocomposite [J]. Journal of Composite Materials, 2015, 49(28): 3507−3514. DOI: 10.1177/0021998314567010.

[7] BAHRAMI A, SOLTANI N, SADRNEZHAAD S K. Manufacturing wear-resistant 10Ce-TZP/Al_2O_3 nanoparticle aluminum composite by powder metallurgy processing [J]. Materials and Manufacturing Processes, 2014, 29: 1237−1244. DOI: 10.1080/10426914.2014.930954.

[8] SAJJADI S A, EZATPOUR H R, BEYGI H. Microstructure and mechanical properties of Al–Al_2O_3 micro and nanocomposites fabricated by stir casting [J]. Materials Science and Engineering A, 2011, 528(29, 30): 8765−8771. DOI: 10.1016/j.msea.2011.08.052.

[9] BARADESWARAN A, ELAYA PERUMAL A. Study on mechanical and wear properties of Al 7075/Al_2O_3 /graphite hybrid composites [J]. Composites Part B, 2014, 56: 464−471. DOI: 10.1016/j.compositesb.2013.08.013.

[10] PANWAR N, CHAUHAN A. Fabrication methods of particulate reinforced aluminium metal matrix composite—A review [J]. Materials Today: Proceedings, 2017, 5(2): 5933−5939. DOI: 10.1016/j.matpr.2017.12.194.

[11] RADHIKA N, SAM M. Tribological and wear performance of centrifuge cast functional graded copper based composite at dry sliding conditions [J]. Journal of Central South University, 2019, 26(11): 2961−2973. DOI: 10.1007/s11771-019-4228-y.

[12] KANDPAL B C, KUMAR J, SINGH H. Manufacturing and technological challenges in stir casting of metal matrix composites—A review [J]. Materials Today: Proceedings, 2018, 5(1): 5−10. DOI: 10.1016/j.matpr.2017.11.046.

[13] AKHLAGHI F, LAJEVARDI A, MAGHANAKI H M. Effects of casting temperature on the microstructure and wear resistance of compocast A356/SiC_p composites: A comparison between SS and SL routes [J]. Journal of Materials Processing Technology, 2004, 155−156: 1874−1880. DOI: 10.1016/j.jmatprotec.2004.04.328.

[14] LIOYD D J. Particle reinforced aluminium and magnesium matrix composites [J]. International Material Review, 1994, 39(1): 1−23. DOI: 10.1179/095066094790150982.

[15] HAN Jian-min, WU Zhao-ling, CUI Shi-hai, LI Wei-jing, DU Yong-ping. Investigation of defects in SiC_p/A356 composites made by a stir casting method [J]. Journal of Ceramic Processing Research, 2007, 8(1): 74−77. DOI: 10.1111/j.1744-7402.2007.02157.x.

[16] MOHANAKUMARA K C, RAJASHEKAR H, GHANARAJA S, AJITPRASAD S L. Development and mechanical properties of SiC reinforced cast and extruded Al based metal matrix composite [J]. Procedia Materials Science, 2014, 5: 934−943. DOI: 10.1016/j.mspro.2014.07.381.

[17] BORREGO A, FERNÁNDEZ R, CRISTINA M D C, IBÁÑEZ J, GONZÁLEZ-DONCEL G. Influence of extrusion temperature on the microstructure and the texture of 6061Al–15 vol.% SiC_w PM composites [J]. Composites Science and Technology, 2002, 62(6): 731−742. DOI: 10.1016/S0266-3538(02)00043-X.

[18] GHANARAJA S, VINUTH KUMAR K, RAJU H P, RAVIKUMAR K S. Processing and mechanical properties of hot extruded Al(Mg)-Al_2O_3 composites [J]. Materials Today: Proceedings, 2015, 2(4, 5): 1291−1300. DOI: 10.1016/j.matpr.2015.07.045.

[19] SOLTANI N, JAFARI NODOOSHAN H R, BAHRAMI A, PECH-CANUL M I, LIU Wen-cai, WU Gou-hua. Effect of hot extrusion on wear properties of Al–15 wt.% Mg_2Si in situ metal matrix composites [J]. Materials and Design, 2014, 53: 774−781. DOI: 10.1016/j.matdes.2013.07.084.

[20] ZHANG Peng-xiang, YAN Hong, LIU Wei, ZHOU Xiu-liang, TANG Bin-bin. Effect of T6 heat treatment on microstructure and hardness of nanosized Al_2O_3 reinforced 7075 aluminum matrix composites [J]. Metals, 2019, 9(1): 44. DOI: 10.3390/met9010044.

[21] DENG Yun-lai, WAN Li, WU Li-hui, ZHANG Yun-ya, ZHANG Xin-ming. Microstructural evolution of Al-Zn-Mg-Cu alloy during homogenization [J]. Journal of Materials Science, 2011, 46(4): 875−881. DOI: 10.1007/s10853-010-

4828-2.

[22] LEI Zhi-bo, ZHAO Ke, WANG Yi-guang, AN Li-nan. Thermal expansion of Al matrix composites reinforced with hybrid micro-/nano-sized Al_2O_3 particles [J]. Journal of Materials Science & Technology, 2014, 30(1): 61−64. DOI: 10.1016/j.jmst.2013.04.022.

[23] MA Ka-ka, WEN Hai-ming, HU Tao, TOPPING T D, ISHEIM D, SEIDMAN D N, LAVERNIA E J, SCHOENUNG J M. Mechanical behavior and strengthening mechanisms in ultrafine grain precipitation-strengthened aluminum alloy [J]. Acta Materialia, 2014, 62: 141−155. DOI: 10.1016/j.actamat.2013.09.042.

[24] NES E. Recovery revisited [J]. Acta Metallurgica et Materialia, 1995, 43(6): 2189−2207. DOI: 10.1016/0956-7151(94)00409-9.

[25] YANG Zi-run, SUN Yu, LI Xin-xing, WANG Shu-qi, MAO Tao-jie. Dry sliding wear performance of 7075 Al alloy under different temperatures and load conditions [J]. Rare Metals, 2015. DOI: 10.1007/s12598-015-0504-7.

[26] RAO R N, DAS S. Effect of matrix alloy and influence of SiC particle on the sliding wear characteristics of aluminium alloy composites [J]. Materials and Design, 2010, 31(3): 1200−1207. DOI: 10.1016/j.matdes.2009.09.032.

[27] WANG Lei, DONG Bai-xin, QIU Feng, GENG Run, ZOU Qian, YANG Hong-yu, LI Qing-yuan, XU Zi-han, ZHAO Qing-long, JIANG Qi-chuan. Dry sliding friction and wear characterization of in situ TiC/Al-Cu3.7-Mg1.3 nanocomposites with nacre-like structures [J]. Journal of Materials Research and Technology, 2020, 9(1): 641−653. DOI: 10.1016/j.jmrt.2019.11.005.

[28] NEMATI N, KHOSROSHAHI R, EMAMY M, ZOLRIASATEIN A. Investigation of microstructure, hardness and wear properties of Al–4.5 wt.% Cu–TiC nanocomposites produced by mechanical milling [J]. Materials & Design, 2011, 32(7): 3718−3729. DOI: 10.1016/j.matdes.2011.03.056.

[29] SAMEEZADEH M, EMAMY M, FARHANGI H. Effects of particulate reinforcement and heat treatment on the hardness and wear properties of AA 2024-$MoSi_2$ nanocomposites [J]. Materials and Design, 2011, 32(4): 2157−2164. DOI: 10.1016/j.matdes.2010.11.037.

[30] YUAN Lin-lin, HAN Jing-tao, LIU Jing, JIANG Zheng-yi. Mechanical properties and tribological behavior of aluminum matrix composites reinforced with in-situ AlB_2 particles [J]. Tribology International, 2016, 98: 41−47. DOI: 10.1016/j.triboint.2016.01.046.

[31] ARCHARD J F. Contact and rubbing of flat surfaces [J]. Journal of Applied Physics, 1953, 24(8): 981−988. DOI: 10.1063/1.1721448.

[32] WILSON S, ALPAS A T. Wear mechanism maps for metal matrix composites [J]. Wear, 1997, 212(1): 41−49. DOI: 10.1016/S0043-1648(97)00142-7.

[33] LIU Wei, YAN Hong, ZHU Jian-bin. Effect of the addition of rare earth element La on the tribological behaviour of AlSi5Cu1Mg alloy [J]. Applied Sciences, 2018, 8(2): 163. DOI: 10.1016/S0043-1648(97)00142-7.

(Edited by HE Yun-bin)

中文导读

热挤压对 Al_2O_{3p} 增强 7075 铝基复合材料微观组织和摩擦学行为的影响

摘要：通过光学显微镜(OM)、扫描电子显微镜(SEM)、能谱仪(EDS)和透射电子显微镜(TEM)研究了热挤压和 Al_2O_{3p} 的添加对 7075 复合材料的微观结构和摩擦学行为的影响。实验结果表明，Al_2O_{3p} 的最佳添加量为 2%(质量分数)。经热挤压后，$Mg(Zn,Cu,Al)_2$ 相部分溶解到基体中，并且产生了许多均匀分布的时效析出颗粒，Al_7Cu_2Fe 相被挤压并破碎，Al_2O_{3p} 分布变得均匀。2%质量分数的 Al_2O_{3p}/7075 复合材料的显微硬度达到 HV 170.34，相比铸态复合材料提高了 41.5%。在相同条件下，挤压态 2%质量分数的 Al_2O_{3p}/7075 复合材料的磨损率比铸态复合材料的磨损率更低。SEM-EDS 分析表明，复合材料耐磨性的增强主要取决于 Al_2O_{3p} 增强的过渡层的保护作用。经过热挤压后，摩擦过渡层变得稳定，这使得挤压态复合材料的耐磨性增强。

关键词：7075 铝合金；Al_2O_{3p}；复合材料；热挤压；微观组织；摩擦学行为